

Internet Electronic Journal of Molecular Design

February 2004, Volume 3, Number 2, Pages 55–72

Editor: Ovidiu Ivanciuc

Special issue dedicated to Professor Nenad Trinajstić on the occasion of the 65th birthday
Part 8

Guest Editor: Douglas J. Klein

Structure of β -Artelinic Acid Clarified Using NMR Analysis, Molecular Modeling and Cyclic Voltammetry, and Comparison with α -Artelinic Acid and β -Arteether

Apurba K. Bhattacharjee,¹ David J. Skanchy,¹ Rickey P. Hicks,¹ Keith A. Carvalho,¹
Gwendolyn N. Chmurny,² John R. Klose,² and John P. Scovill²

¹ Department of Medicinal Chemistry, Division of Experimental Therapeutics, Walter Reed Army
Institute of Research, 503 Robert Grant Avenue, Silver Spring, MD 20910

² Chemical Synthesis and Analysis Laboratory, SAIC Frederick, MD

Received: July 9, 2003; Revised: October 15, 2003; Accepted: November 14, 2003; Published: February 29, 2004

Citation of the article:

A. K. Bhattacharjee, D. J. Skanchy, R. P. Hicks, K. A. Carvalho, G. N. Chmurny, J. R. Klose,
and J. P. Scovill, Structure of β -Artelinic Acid Clarified Using NMR Analysis, Molecular
Modeling and Cyclic Voltammetry, and Comparison with α -Artelinic Acid and β -Arteether,
Internet Electron. J. Mol. Des. **2004**, *3*, 55–72, <http://www.biochempress.com>.

Structure of β -Artelinic Acid Clarified Using NMR Analysis, Molecular Modeling and Cyclic Voltammetry, and Comparison with α -Artelinic Acid and β -Arteether[#]

Apurba K. Bhattacharjee,^{1,*} David J. Skanchy,¹ Rickey P. Hicks,¹ Keith A. Carvalho,¹ Gwendolyn N. Chmurny,² John R. Klose,² and John P. Scovill²

¹ Department of Medicinal Chemistry, Division of Experimental Therapeutics, Walter Reed Army Institute of Research, 503 Robert Grant Avenue, Silver Spring, MD 20910

² Chemical Synthesis and Analysis Laboratory, SAIC Frederick, MD

Received: July 9, 2003; Revised: October 15, 2003; Accepted: November 14, 2003; Published: February 29, 2004

Internet Electron. J. Mol. Des. 2004, 3 (2), 55–72

Abstract

A detailed analysis on the structure of β -artelinic acid has been performed using proton, carbon-13, 1D and 2D NMR, molecular modeling, and cyclic voltammetry methods. The results are compared by carrying out similar experiments and modeling studies with α -artelinic acid and β -arteether. Certain critical non-bonded interactions between specific protons and the ether oxygen atom in the neighborhood of the anomeric carbon atom seem to be particularly significant in the two isomers. Although the stereochemistry at the anomeric carbon atom in the sesquiterpene skeleton of these molecules is diastereomeric, the structural difference between α and β isomers and *ab initio* quantum chemical calculations on these compounds (using both RHF/3-21G* and RHF/6-31G** basis sets) indicate significant difference in the mode of interaction of the neighboring protons by this atom. The difference in these interactions accounts for the observed difference in NMR chemical shifts of the protons in the two isomers. The peroxide oxygen atoms in the diastereomers do not appear to be significantly affected by these protons and the intrinsic nucleophilicity of the peroxide oxygen atoms remain almost unchanged as evidenced from the calculated electrostatic potentials on these atoms and redox potentials determined by cyclic voltammetry experiments. Calculated (HF/6-31G**/NMR) chemical shift values are found to be consistent with the trends of the experimental values. The present combined NMR chemical shift assignments, molecular modeling and cyclic voltammetry study focuses the role of electronic distribution by the aromatic ring in the two isomers in relation to the protons around the anomeric carbon atom in the sesquiterpene skeleton to affect the activity of the isomers. The results should aid in the design of new artemisinin analogues with potent activity and reduced CNS toxicity.

Keywords. Malaria; β -artelinic acid; NMR; *ab initio* 6-31G** basis set; cyclic voltammetry.

1 INTRODUCTION

Artemisinin and its derivatives are promising new antimalarials for the treatment of multidrug resistant *Plasmodium falciparum*, particularly for chloroquine and mefloquine resistant areas of the malaria endemic regions of the world. The antimalarial activity of the compounds appears to be

[#] Dedicated to Professor Nenad Trinajstić on the occasion of the 65th birthday.

* Correspondence author; E-mail: Apurba.Bhattacharjee@na.amedd.army.mil.

mediated through an interaction of the endoperoxide moiety and intraparasitic heme, producing free radicals that may be responsible for killing the parasite [1]. The endoperoxide bond is necessary for antimalarial activity since deoxy derivatives are inactive. However there are a few shortcomings of artemisinin such as its high rate of recrudescence, poor solubility in oil and water, short plasma half-life, and poor oral activity that limit the practical utility of this compound as a drug. In order to overcome the practical difficulties, several chemical modifications of artemisinin were made and a number of analogs with improved efficacy and increased solubility such as arteether, artemether, sodium artelinate and sodium artesunate were discovered [2]. Artemether and arteether showed higher potency than artemisinin but were found to have shorter plasma half-lives and exhibited neurotoxicity in rats and dogs. The usefulness of sodium artesunate too is offset by problems associated with its rapid hydrolysis in aqueous medium, its high rate of recrudescence and extremely short plasma half-life [2]. However, sodium artelinate could not only overcome the aqueous solubility problem of sodium artesunate but also has a much longer plasma half-life than the three other artemisinin analogs. Furthermore, the neurotoxicity studies on sodium artelinate indicate lessened CNS toxicity in rat and dog than oil soluble analogs such as artemether and arteether. It is commonly believed that these compounds are converted by enzymatic hydroxylation to dihydroartemisinin (DQHS) by cytochrome P-450 [3]. Plasma half-life of these derivatives is dependent on the oxidative dealkylation or deacylation which generates DQHS. Continued efforts for finding safer analogs of artemisinin led to the discovery of artelinic acid. Interestingly, artelinic acid has a longer plasma-half life than those three analogs probably due to its slower rate of dealkylation to DQHS. However, since the stereochemistry at C10 position of artelinic acid can result in the formation of two isomers, α and β (Chart A), understanding the structural features of artelinic acid should provide better insights for designing new analogs that will have better solubility, longer plasma half life, and higher antimalarial potency than artemisinin and lesser CNS toxicity. NMR studies on ethyl 3(R and S)-(p-nitrophenyl)-3-(10 β -dihydroartemisininoxy) propionate, a derivative of artelinic acid, have shown large differences in the chemical shift pattern of the two protons adjacent to the ether linkages of two of its diastereomers [4]. The crystal structures of the two diastereomers (one as the ethyl ester and the other as the acid analog) also showed two oppositely positioned nitrophenyl groups in the fused ring system of the two diastereomers.

In the present study we have completely assigned the ^1H and ^{13}C chemical shifts of β -artelinic acid (Chart A, 2) and compared it to the ^1H and ^{13}C chemical shifts of α -artelinic acid [5] (Chart A, 1) and β -arteether (Chart A, 3) by proton and carbon-13, 1D and 2D NMR spectroscopy. Computational studies based on *ab initio* quantum chemical calculations are performed at Restricted Hartree-Fock (RHF) level using both 6-31G** and 3-21G* basis sets on the three compounds to better understand the intra-molecular forces governing the structure-function relationship of the two anomers and to interpret the observed NMR spectral results. In addition, we have examined

peroxide bond strengths in these compounds using cyclic voltammetry methods to correlate structural differences to the observed differences in the antimalarial activity of the compounds.

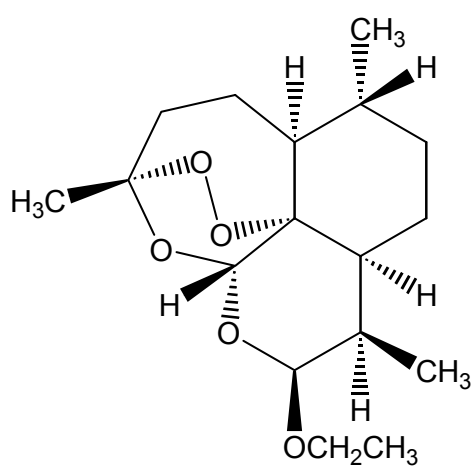
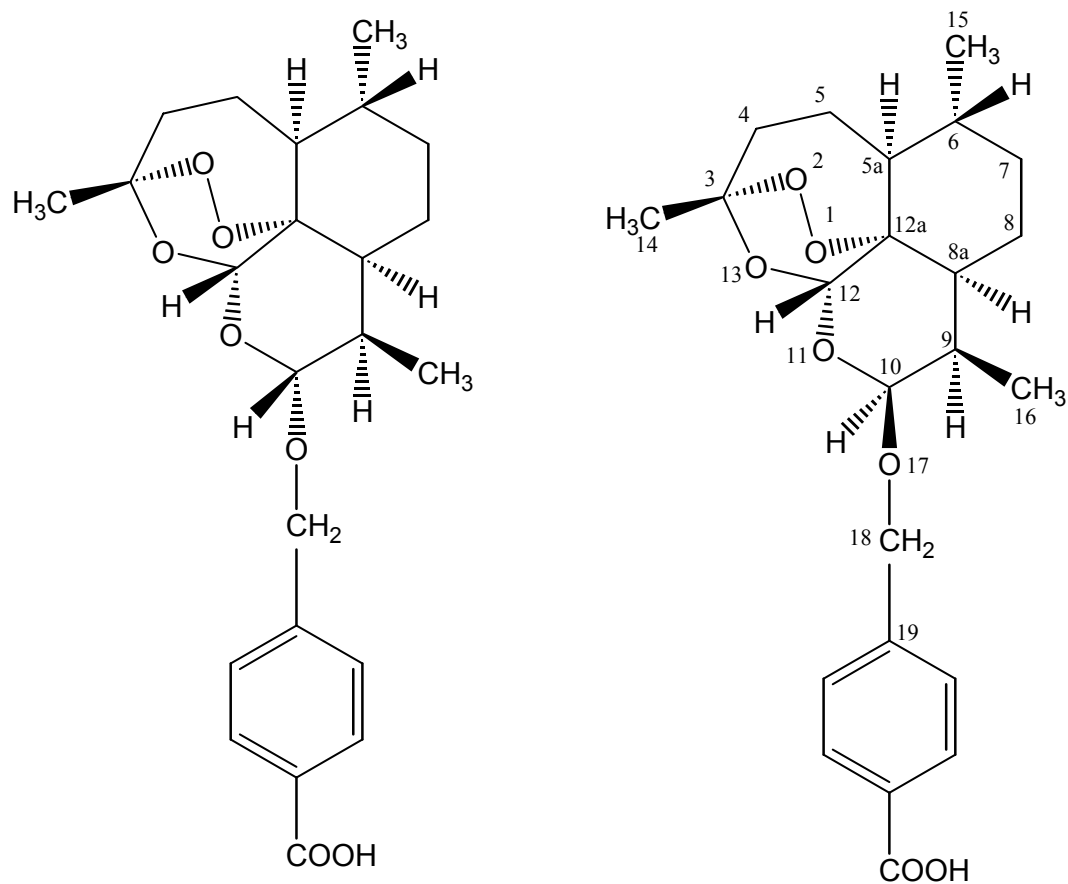


Chart A

2 MATERIALS AND METHODS

2.1 Chemical Data

2.1.1 NMR spectra

Samples for analysis in CDCl_3 were prepared as follows. 8.5 mg of β -artelinic acid was dissolved in 150 μL of CDCl_3 . 9 mg of α -artelinic acid and 10 mg of β -arteether were dissolved separately in 150 μL of CDCl_3 . In addition, the proton and carbon-13 spectra of 5.0 mg of β -artelinic acid was assigned in D_2O to illustrate the effect of solvent on chemical shift values.

1D and 2D proton and carbon-13 NMR spectra were collected using a Bruker DRX-600 spectrometer operating at a proton frequency of 600.06 MHz and a carbon frequency of 150.90 MHz and using a Varian VXR500S/UNITY 500 MHz spectrometer equipped with a Nalorac 3mm probe. Proton spectra were acquired using 16 scans with a spectral width of 12376 Hz, using 64k data points. The spectrum was processed with exponential multiplication using a line-broadening factor of 0.3 Hz. The 2D COSY spectrum was collected with a spectral width of 3004 Hz using 2K data points with 16 scans per 512 t_1 increments with a 1 s recycle delay. The data set was processed by multiplying a 90° shifted sine-bell window function in each dimension before transformation to produce matrices consisting of 1024 data points in both dimensions.

2D ^1H - ^{13}C HMQC and HMBC [6] spectra were collected with a spectral width of 3004 Hz in the proton dimension and 8012 Hz in the carbon-13 dimension using 2K data points with 64 scans per 512 t_1 increments with a 1.5 s recycle delay. Data obtain from both experiments were processed by multiplied by a 90° shifted sine-bell window function in each dimension before transformation to produce matrices consisting of 1024 data points in both dimensions.

Carbon-13 spectra were collected with a spectral width of 37593 Hz using 64K data points a total of 10 k scans were collected. Data were processed using exponential multiplication with a line broadening of 1.0 Hz.

2.1.2 Biological activity

The compounds were examined for IC_{50} values against the *P. falciparum* W2 (Indochina) and D6 (Sierra Leone) clones in vitro. The in vitro assays were conducted by using the semiautomated microdilution technique of Desjardins *et al.* [7] and Chulay *et al.* [8]. The W2 clone is susceptible to mefloquine but resistant to chloroquine, sulfadoxine, pyrimethamine, and quinine. The D6 clone is resistant to mefloquine but susceptible to chloroquine, sulfadoxine, pyrimethamine, and quinine. The clones were derived by direct visualization and micromanipulation from the patient isolates. Test compounds were initially dissolved in DMSO and diluted 400-fold in RPMI 1640 culture medium supplemented with 25mM HEPES, 32 mM NaHCO_3 and 10% Albumax I (GIBCO BRL, Grand Island, NY). These solutions were subsequently serially diluted 2-fold with a Biomek 1000 (Beckman, Fullerton, CA) over 11 different concentrations. The parasites were exposed to serial

dilutions of each compound for 48 h and incubated at 37°C with 5% O₂, 5% CO₂, and 90% N₂ prior to the addition of [³H]hypoxanthine. After a further incubation of 18 h, parasite DNA was harvested from each microtiter well using Packard Filtermate 196 Harvester (Meriden, CT) onto glass filters. Uptake of [³H]hypoxanthine was measured with a Packard topcount scintillation counter. Concentration–response data were analyzed by a nonlinear regression logistic dose–response model, and the IC₅₀ values (50% inhibitory concentrations) for each compound were calculated. Table 6 shows the results of the W2 clones, D6 results parallel the W2 results.

2.1.3 Cyclic voltammetry

Cyclic voltammetry experiments were performed on a CV–50W voltammetric analyzer with a C2 cell stand (Bioanalytical systems, West Lafayette IN). A glassy carbon working electrode, a silver-silver chloride reference electrode and a platinum auxiliary electrode were used in a 5 mL glass cell. All samples were dissolved in 60% phosphate buffered saline (0.14 M NaCl, 0.008 M Na₂HPO₄, 0.002 M NaH₂PO₄, pH 7.3) and 40% ethanol (Aldrich, St. Louis, MO). Each of the three artemisinins was prepared at a concentration of 1 mM and was degassed with nitrogen for five minutes prior to analysis. Samples were run at several scan rates ranging from 20 to 1000 mV/sec as per the reported procedure [9]. Instrument IR compensation was used to compensate for solution resistance in all experiments.

2.2 Computer Software

Initially, a conformational search analysis of the compounds was performed using the systematic conformational search techniques in SPARTAN [10] at the AM1 single point level to obtain the population of low energy conformers. Monte Carlo “simulated annealing” approach as implemented in SPARTAN [10] was also used to generate trial conformations by way of random bond and ring torsions. Initially, the molecule is considered to be in a high temperature system i.e., it has sufficient energy to move from low to high energy conformations. This is important because often the global minimum conformation remains hidden by many local minima. As more conformations are explored, the temperature is decreased, making the molecule less able to move out of low energy conformations. Thus, when the search is completed, the molecule is most likely to be in the lowest energy conformation found up to that point. The global minimum–energy of the conformers identified by both the above methods are compared and assessed. In this way the lowest and the most abundant (highest population density) energy conformer was selected for subject to complete geometry optimization by using RHF/3-21G* split valence and subsequently, RHF/6-31G** basis sets in Gaussian94 [11] running on a SGI Octane workstation. The electronic properties such as molecular electrostatic potentials and orbital energies were calculated on the optimized geometry of the molecule.

Molecular electrostatic potentials (MEPs) were sampled over the entire accessible surface of the

molecule (surface of a constant 0.002 e/au^3 electron density corresponding roughly to a van der Waals contact surface), providing a measure of charge distribution from the point of view of an approaching reagent. The regions of positive electrostatic potential indicate excess positive charge, *i.e.*, repulsion for the positively charged test probe, while regions of negative potential indicate areas of excess negative charge, *i.e.*, attraction of the positively charged test probe. These isosurface values provide an indication of overall molecular size and of location of negative or positive electrostatic potentials.

For example, in the present study, the MEPs encoded onto a surface of constant electron density (0.002 e/au^3) portrays both steric and MEP characteristics of the molecules. This encoding is done by the use of color, colors toward the blue representing one extreme value of a property (most electrophilic being deepest blue) and colors toward the red representing the other extreme (deepest red being the most nucleophilic). Isopotential surfaces extending outward from the van der Waals surface of each molecule at -40 and -10 kcal/mol were also generated to indicate the electron density profiles beyond molecular surface. NMR chemical shielding tensors were evaluated employing the GIAO (Gauge-Independent Atomic Orbital) method at RHF/6-31G** optimized geometry of each of the compounds as implemented in Gaussian94 [11]. We have calculated the chemical shift of TMS at the same level of theory as for the compounds and then calculated the difference between the chemical shift for the molecule and the TMS as the relative chemical shift in the line with previously reported procedures [12,13].

3 RESULTS AND DISCUSSION

3.1 NMR Analysis

Proton and carbon-13 chemical shift assignments are shown in Tables 1–4. 1D and 2D proton and carbon-13 spectra were used to assign the proton and carbon-13 chemical shifts for the β and α isomers of artelinic acid as well as for arteether. An example of how the 2D ^1H - ^{13}C HMQC and HMBC spectra were used [14,15] to assign the complete carbon-13 spectrum of β -artelinic acid is given in Figure 1.

The stereochemistry at C10 is the only structural difference between the β and α isomers of artelinic acid. Arteether is a β conformer. The structural difference at the C10 position is determined by the $^3J_{\text{CH}}$ between H9 and H10 protons. A large difference in this coupling constant is observed: $^3J_{\text{CH}}$ is 3.4 and 9.2 Hz in the β and α isomers, respectively. The proton chemical shifts differ significantly between the β and α isomers of artelinic acid (Table 1). The shifts from α to β to higher frequency occur for H9 and H11 and to a lesser extent for 8CH_{2a} and to lower frequency for H10 and 7CH_{2b} and still to a lesser extent for H6 and H8a. Corresponding carbon chemical shift assignments for the two anomers are given in Table 2 and 3.

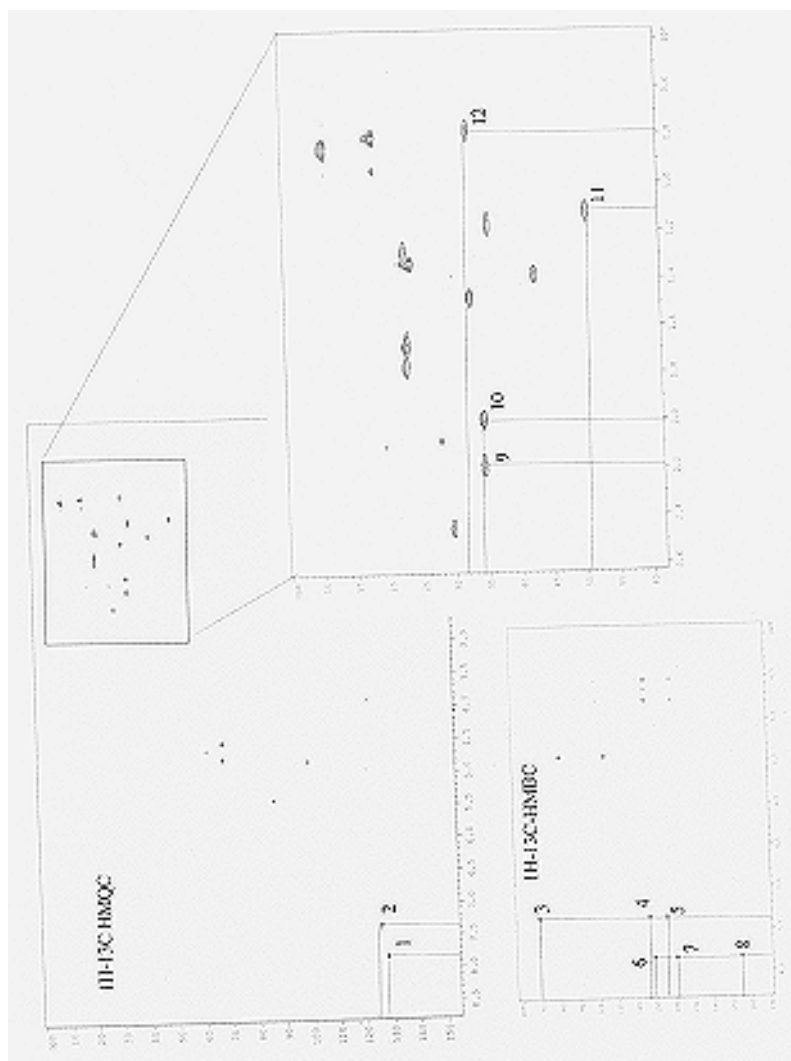


Figure 1. Illustration of the interactive use of the ^1H - ^{13}C -HMBC and ^1H - ^{13}C -HMQC spectra to assign the carbon spectrum of b-artelinic acid in D_2O . ^1H - ^{13}C connectivity 1) m-CH= to m-CH, 2) o-CH= to o-CH, 3) o-CH= to BzCH₂, 4) o-CH= to m-CH, 5) o-CH= to iC, 6) m-CH= to 7) m-CH= to iC, 8) m-CH= to ArCOOH, 9) 4CH₂a to 4CH₂, 10) 4CH₂b to 4CH₂, 11) H6 to C6, 12) 6-CH₃ to 6-CH₃.

In the carbon-13 spectrum, the shifts from α to β to higher frequency occur for C10 and C8 and to a lesser extent for C7 and C6a and to lower frequency for C11 and C9 and to a lesser extent for C8a. The proton chemical shift differences (Table 1) between beta artelinic acid (I) and beta arteether (III) in which the stereochemistry at C10 is unchanged and the substituent at C10 has changed from O-benzyl to O-ethyl show mostly high frequency shifts (O-benzyl to O-ethyl) for H9, 8CH₂b, 3Me, and 9Me and to a lesser extent for H11, H8a and H6a. There is only one large low frequency shift for H10 and a lesser one for H8a. As expected, the carbon-13 chemical shifts (O-benzyl to O-ethyl) change only slightly, a small high frequency shift for C8 and a small low frequency shift for C8a. The chemical shifts for the H9 proton in α -artelinic acid occurs at lower field (2.54 ppm) than the H9 proton in β -artelinic acid (2.71 ppm). The shifts for the H11 protons follow the same pattern with the H11 proton in the α anomer occurring at 6.36 ppm and that of the β anomer occurring at 5.41 ppm.

Table 1. ^1H NMR Chemical Shift Assignments (ppm) for β -Artelinic acid in D_2O and CDCl_3 and α -Artelinic acid and β -Arteether in CDCl_3

Assignment	β -Artelinic acid		α -Artelinic acid	β -Arteether acid
	D_2O	CDCl_3	CDCl_3	CDCl_3
<i>m</i> -CH= ^a	7.81	8.10	8.08	–
<i>o</i> -CH= ^a	7.33	7.43	7.47	–
H12	5.46	5.47	5.36	5.41
BzCH ₂ a	4.82	4.99	5.06	OCH ₂ a 3.86
H10	4.81	4.94	4.71	4.80
BzCH ₂ b	4.58	4.61	4.54	OCH ₂ b 3.47
H9	2.51	2.71	2.54	2.61
H4	2.23	2.39	2.40	2.37
H4	2.07	2.05	2.04	2.03
H5	1.36	1.89	1.89	1.88
H8	1.86	1.84	1.74	1.84
H8	1.77	1.83	1.67	1.74
H7	1.44	1.65	1.58	1.63
H8a	1.47	1.50	1.49	1.45
H5	1.18	1.49	1.47	1.50
14-CH ₃	1.39	1.46	1.31	1.44
H6	1.24	1.33	1.27	1.34
H5	1.35	1.27	1.22	1.24
16-CH ₃	0.91	0.98	1.01	0.90
15-CH ₃	0.87	0.95	0.96	0.95
H7	0.85	0.93	0.95	0.91

^a defines position as either *o*- (orto) or *m*- (meta) to the carboxylic acid moiety

Table 2. Comparison of the observed ^{13}C Chemical Shifts Assignments (ppm) for β -Artelinic acid in D_2O and CDCl_3 to Calculated Values

Assignment	β -Artelinic acid		
	D_2O	CDCl_3	calculated
ArCOO ₂ H	175.8	171.7	157.3
<i>i</i> C ^a	141.3	144.6	146.2
<i>m</i> CH ^a	128.2	130.3	125/124
<i>p</i> C ^a	127.6	128.3	129.0
<i>o</i> CH ^a	126	126.9	125/123
C3	105	104.2	90.1
C10	100.4	101.7	88.4
C12	87.0	88.0	77.2
C12a	82.0	81.1	44.1
BzCH ₂	68.4	69.20	60.7
C6a	51.1	52.5	45.0
C8a	43.1	44.3	38.6
C6	32.7	37.4	31.5
C4	34.8	36.4	33.2
C7	33.1	34.6	30.8
C9	29.8	30.9	28.0
C14	24.2	26.13	25.8
C5	–	24.6	23.2
C8	23.2	24.5	21.6
C15	11.3	20.3	19.8
C16	18.6	13.1	14.4

^a defines the position of the carbon atom in the benzene ring relative to the point of attachment to the ring. *i* = point of attachment, *o* = orto, *m* = meta, *p* = para

Table 3. Comparison of the observed and calculated ^{13}C chemical shifts assignments (ppm) for α -artelinic acid in CDCl_3

Assignment	α -Artelinic acid	
	CDCl_3	calculated
ArCOO_2H	171.8	160.3
$i\text{C}^a$	144.6	148.4
$m\text{CH}^a$	130.2	126.2/124.4
$p\text{C}^a$	128.3	124.4
$o\text{CH}^a$	127.2	131.9/134.3
C3	104.4	90.3
C10	99.2	85.1
C12	91.3	79.9
C12a	80.3	69.9
BzCH_2	69.2	55.9
C6a	51.6	44.3
C8a	45.3	39.3
C6	37.3	31.6
C4	36.3	33.1
C7	34.1	30.7
C9	32.7	27.0
C14	26.0	25.7
C5	24.7	23.3
C8	22.2	19.9
C15	20.2	19.8
C16	12.7	13.9

^a defines the position of the carbon atom in the benzene ring relative to the point of attachment to the ring; *i* = point of attachment, *o* = orto, *m* = meta, *p* = para

Table 4. Comparison of the Observed ^{13}C Chemical Shifts Assignments (ppm) for β -Arteether in CDCl_3 to Calculated Values

Assignment	β -Arteether	
	CDCl_3	calculated
C3	104.0	89.8
C10	101.6	88.5
C12	87.9	77.1
C12a	81.1	70.4
OCH_2	63.7	55.7
C6a	52.6	45.1
C8a	44.5	38.8
C6	37.4	31.6
C4	36.4	33.4
C7	34.6	31.0
C9	30.8	27.9
C14	26.2	25.9
C5	24.7	23.3
C8	24.4	21.6
C15	20.3	20.0
OCH_2CH_3	15.1	16.8
C16	13.0	14.3

3.2 Molecular Modeling

The calculated and the experimental NMR chemical shift values show remarkable consistency in trends and clearly help in explaining the differences between the α and β isomers. A comparison of the calculated nonbonded distances between the hydrogens of C8, C8a, C9 and C10 and the two oxygen atoms O1 (peroxide) and O17 (ether) are shown in (Table 5). The results of the quantum chemical calculations are discussed in the light of the following two sections.

Table 5. Selected RHF/3-21G* and RHF/6-31G** energies, distances, dihedral angles, and negative electrostatic potential values of the compounds

Parameter	α -artelinic acid		β -artelinic acid		β -arteether	
	3-21G*	6-31G**	3-21G*	6-31G**	3-21G*	6-31G**
Total energy (hartrees)	-1404.60816	-1412.45759	-1404.59807	-1412.45021	-1028.59759	-1034.32325
Peroxide bond length (Å)	1.463	1.392	1.463	1.392	1.463	1.392
Nonbonded distance (Å)						
H8 ^a ...O1	2.479	2.441	2.44	2.424	2.433	2.422
H8 ^a ...O17	4.54	4.545	4.031	4.065	4.018	4.06
H8 _{ax} ...O1	4.518	4.488	4.504	4.482	4.501	4.481
H8 _{ax} ...O17	4.777	4.715	3.302	3.436	3.303	3.433
H8 _{ax} ...C19	6.3	7.041	3.7	5.04	3.6	4.741
H8 _{eq} ...O1	4.178	4.194	4.196	4.203	4.202	4.204
H8 _{eq} ...O17	4.268	4.150	2.328	2.432	2.292	2.421
H8 _{eq} ...C19	6.21	6.474	4.8	3.83	4.8	3.548
H9...O1	2.399	2.509	2.437	2.510	2.458	2.518
H9...O17	2.608	2.678	3.303	3.275	3.299	3.273
H10...O1	4.299	4.233	4.091	4.102	4.11	4.108
H10...O17	1.997	1.957	2.057	2.027	2.058	2.026
H10...C19	2.955	4.26	4.004	3.945	4.023	4.090
Dihedral angle (°)						
C10-O17-C18-C19	114.3	-146.3	176.4	178.2	-179.6	178.0
H10-C10-O17-C18	165.3	175.0	-53.6	-50.1	-49.9	-47.8
C9-C10-O17-C18	-73.3	-64.3	-175.5	-170.9	-171.9	-168.7
MEP values (kcal/mol)						
Peroxide bond	-37.0	-30.6	-40.0	-29.5	-45.0	-33.5

3.2.1 Steric attributes

At both the basis set levels (RHF/3-21G* and RHF/6-31G**), the optimized geometry of the two anomers of artelinic acid and β -arteether is found to have a fully saturated D ring in a chair conformation with equatorial α substituents and axial β substituents in agreement with the reported crystal structures of some of the artemisinin analogs [16]. Semi-empirical AM1 optimized geometry of the compounds agrees poorly with crystallographic result [17], and are particularly inaccurate about the peroxide bond. This demonstrates the necessity to optimize geometry at a higher level of theory. Experimental studies indicate that the peroxide bond distance in the artemisinin compounds to be around 1.47 Å [16]. However, it is interesting to note that 6-31G** basis set produced a smaller peroxide bond length (1.392 Å) than the 3-21G* basis set (1.463 Å) in the optimized geometry of the anomers. Thus apparently, 3-21G* geometry of the molecules conform better to the experimental structure and does not show any improvement with higher basis sets [18,19]. However, electron correlation must be important for accurate representation of the

peroxide bond. Since electron correlation computations are lengthy and it was not the focus of our present study, we have carried out computations using both the basis sets to check the basis set dependence of other calculated stereoelectronic properties, such as nonbonded distances, dihedral angles and the electrostatic potentials over the peroxide bond (Table 5) and to cross validate the calculated NMR chemical shifts. The optimized structures of the three compounds are presented in Figure 2. The difference in total *ab initio* energy between α - and β -artelinic acid is 6.3 kcal/mol at 3–21G* level and 4.6 kcal/mol at 6–31G** level, respectively, and the α isomer is found to be intrinsically more stable at both levels of theory. However, since the β isomer is always the predominant product it may be plausible to speculate the reaction path be controlled kinetically rather than thermodynamically.

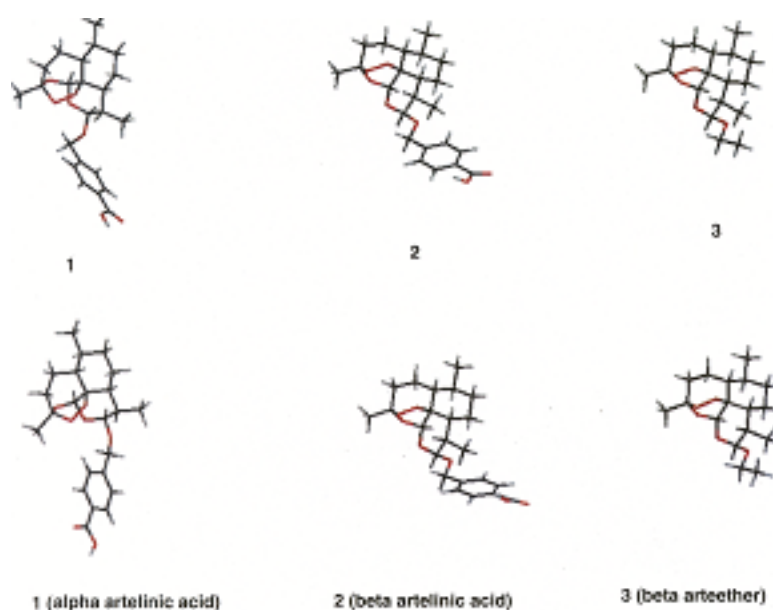


Figure 2. Optimized geometry of the compounds at 3–21G* (top row) and 6–31G** (bottom row) levels of *ab initio* quantum chemical theory.

Since the stereochemistry of the anomeric carbon atom, C10 is the only significant structural difference between the two isomers we have examined the properties of the anomers more extensively surrounding this atom. Inspection of Table 5 indicates that the calculated nonbonded distances and structural features related to the trioxane ring in β -artelinic acid and β -arteether are almost identical. Superimposed optimized structures of β -artelinic acid and β -arteether are presented in Figure 3. However, some of these distances such as, H8_{axial} ..O17, H8_{eq} ..O17, H9 ..O17, H8a .. O17 and H9 .. O1 differ significantly from the α to the β isomer in both artelinic acid and β -arteether. Both H8_{ax} and H8_{eq} protons in β -artelinic acid are significantly closer to the O17 atom, by 1.4 Å and 1.9 Å (3–21G*), respectively. The 6–31G** level calculations are found to be consistent where the H8_{ax} and H8_{eq} protons are 1.28 Å and 1.72 Å closer to the O17 atom, respectively, in β -artelinic acid. The distance between O17 and H8a proton in the β isomers is about 0.5 Å closer than the α -artelinic acid, whereas, the distances from the H9 proton in β -

artelinic acid and β -arteether are about 0.7 Å (3-21G* basis set) and 0.6 Å (6-31G** basis set), respectively, away from the O17 atom. However, the nonbonded distance between the H10 proton and O1 or O17 does not show any significant difference in the anomers. Remarkably, the calculated distance between peroxide O1 atom and H8_a, H8_{ax}, H8_{eq}, H9, and H10 protons remain almost unaltered in both the anomers at both levels of theory, an observation found to be consistent with the cyclic voltammetry experiments on the compounds to be discussed in a later section. The dihedral angles, C10–O17–C18–C19, H10–C10–O17–C18, and C9–C10–O17–C18 differ significantly between the α and the β isomers of artelinic acid and arteether, though they are nearly identical in β -arteether and β -artelinic acid (Table 5, Figure 3).

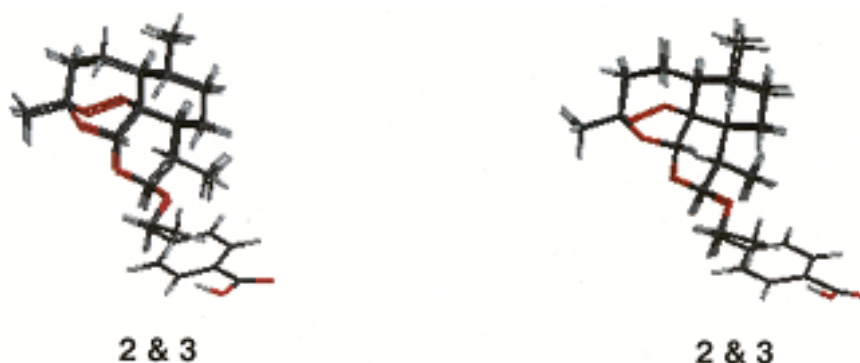


Figure 3. Superimposition of the optimized geometry of β -artelinic acid and β -arteether at 3-21G* level (left) and 6-31G** (right).

Thus, the interaction between the protons in the neighborhood of C10 atom and particularly the ether oxygen atom (O17) in the β isomers is significantly different. The NMR chemical shift values too reflect large differences. The observed $^3J_{\text{CH}}$ between H9 and H10 are 3.4 and 9.2 Hz in the β and the α isomers, respectively. Shorter calculated nonbonded distances between H9 and O17 in the α isomer probably indicates a stronger interaction in the α isomer than the β isomer and thus accounts for the lower field (Table 1–4). Moreover, a dramatic difference in the calculated nonbonded distance is observed between the H8_{ax} proton and C19 atom of the aromatic ring in the two isomers (Table 5). The H8_{ax} in the α - isomer is about 2.6 Å (3-21G*) and 2.0 Å (6-31G**) away from the aromatic ring than the β - isomer of artelinic acid and arteether. The H8_{eq} in the α isomer is also about 1.4 Å (3-21G*) and 2.6 Å (6-31G**) away from the aromatic ring than the β isomer of artelinic acid and arteether. Thus, both these two protons in α -artelinic acid are likely to be more deshielded and chemical shift values clearly reflect this effect (Table 1–4). Large differences in the dihedral angles by O17 atom between the α and β isomers may be attributed to a similar type of interaction (Table 5). Therefore, the closer proximity of H8_{ax} and H8_{eq} protons to the aromatic ring in β -artelinic acid as observed from calculations is clearly consistent with the NMR derived chemical shift values of the two protons. Thus, the steric attributes indicate that the aromatic ring in β -artelinic acid is likely to have a different effect in the surrounding of O17 atom than its α anomer in the structure function relationships of these two compounds.

3.2.2 Electronic attributes

Molecular electrostatic potentials (MEPs) of the accessible surface (roughly onto a 0.002 e/au^3 electron isodensity) of the three compounds were computed and plotted (Figure 4). Inspection of the figure indicates that all the three compounds have negative potential region (red color) by the peroxide bond but the most negative potential region (deepest red) in the two acids is localized by the carbonyl oxygen atom of the acid moiety unlike the arteether where it is localized by the ether oxygen atom (Figure 4).

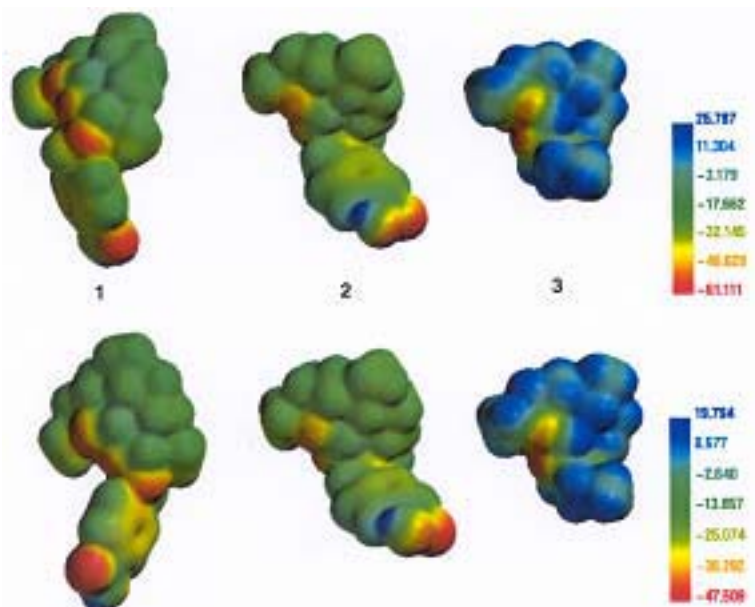


Figure 4. Molecular electrostatic potential (MEP) profiles of the compounds. Top: 3–21G* level; Bottom: 6–31G** level.

However, the positive potential regions (blue color) differ dramatically from the two anomers of artelinic acid and arteether. The positive potential appears to be spread over a large region in β -arteether making it probably more hydrophobic than the two artelinic acid anomers which could be a contributing factor for its observed neurotoxicity in animals [20]. Widely distributed weak positive electrostatic field regions on the accessible molecular surface are believed to be an indication of hydrophobicity of a molecule which is supposedly linked to neurotoxicity [21]. The α -artelinic acid appears to have a different electron density and electrostatic profile than the β isomer (Figure 4). The negative potential region by the peroxide bond in the α isomer appears to have merged with the ether oxygen atom O13 forming a greater extended negative potential region in this part of the molecule. The molecular surface of the α isomer also indicates a different steric feature that is likely to have a different orientation for binding with the receptor than the β isomer. The magnitude of negative potential over the peroxide bond differs marginally between α -artelinic acid (-37.0 kcal/mol), β -artelinic acid (-40.0 kcal/mol), and β -arteether (-45.5 kcal/mol). The small difference of negative electrostatic potential by the peroxide bond indicates that the intrinsic nucleophilicity of the peroxide bond in the two artelinic acids remains virtually unaffected due to

the anomeric isomerism. However, the electronic distribution elsewhere in the molecule is quite significant due to the anomeric effect between the α and β isomers that are clearly noticeable in the three-dimensional electrostatic potential profiles beyond the van der Waals surface at -40 kcal/mol (Figure 5) and -10 kcal/mol (Figure 6).

The potential profile at -40 kcal/mol shows the orientation of the lone pair electrons by the oxygen atoms in these compounds (Figure 5) and the difference in the electronic distribution by the trioxane ring.

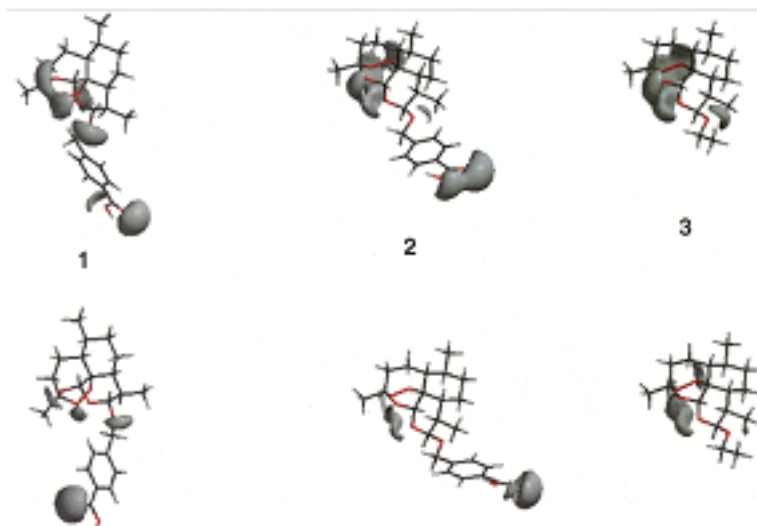


Figure 5. Electrostatic potential maps at -40 kcal/mol showing electronic distribution beyond the van der Waals surface of the molecules. (Top: RHF/3-21G*; Bottom: RHF/6-31G**).

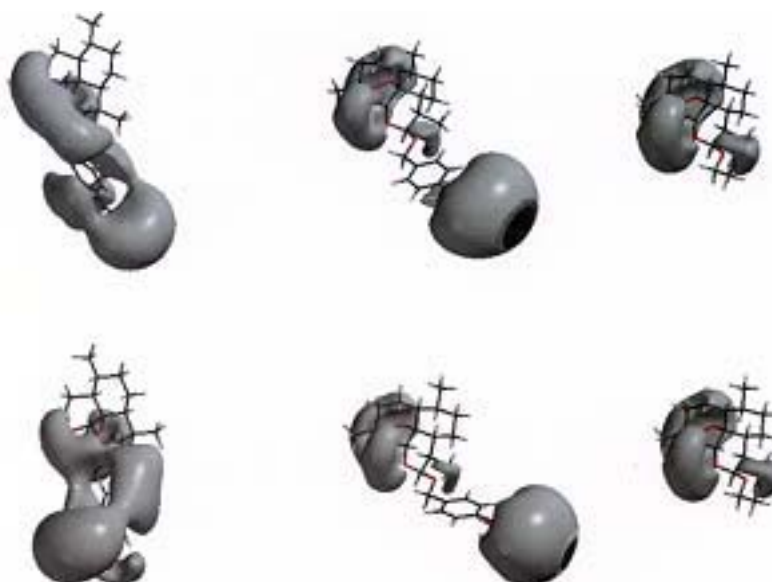


Figure 6. Electrostatic potential maps at -10 kcal/mol showing electronic distribution approximately 1.4 Å away from the van der Waals surface of the molecules (Top: RHF/3-21G*; Bottom: RHF/6-31G**).

The electronic distribution over the trioxane ring in β -arteether is more extended around the peroxide bond (Figure 6) and clearly similar to β -artelinic acid but substantially different from the α -artelinic acid (Figure 5 and 6). The large difference in chemical shift values of H_{8ax} and H_{8eq} protons between the α and β isomers may be attributed to effects upon the protons due to this large difference in the electronic distribution.

3.3 Cyclic Voltammetry

The cyclic voltammograms of α - and β -artelinic acids and β -arteether are shown in Figure 7. A comparison of the reduction potential values, antimalarial activity and available neurotoxicity data of the compounds are presented in Table 6. A single cathodic peak is observed for both isomers of artelinic acid (Figure 7) and β -arteether (data not shown) with no occurrence of an anodic peak, indicating an irreversible reduction. Artemisinin compounds are known to show single irreversible peak in the cyclic voltammogram [22].

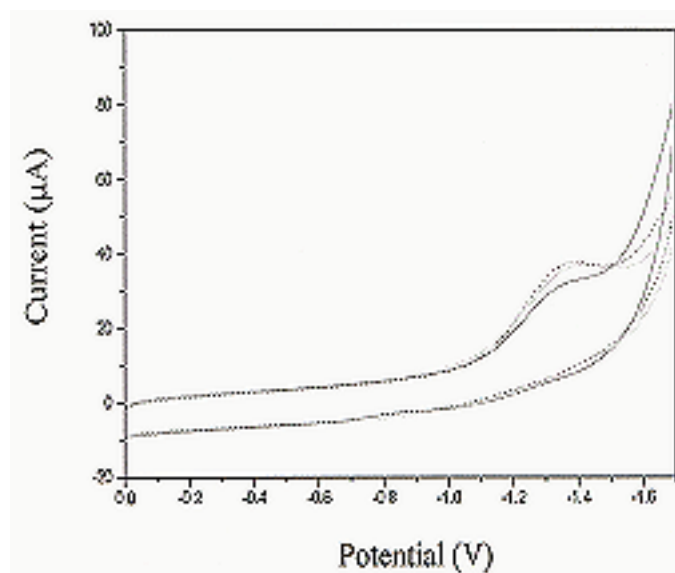


Figure 7. Cyclic voltammogram of 1 mM α -artelinic acid (dashed line) and 1 mM β -artelinic acid (solid line) at 0.4 V/sec scan rate.

Table 6. Comparison of the redox potentials of the compounds with antimalarial activity and neurotoxicity

Compound	Redox Potentials (in V, volts)	Antimalarial Activity IC-50 (nM) ^a	Relative Neurotoxicity ^b
α -artelinic acid	-1.36	18.7	NA ^c
β -artelinic acid	-1.37	15.1	1.5
β -arteether	-1.37	4.1	8.9

^a ref. [7, 8]

^b A value of 1.0 indicates no neurotoxicity at the highest dose tested (100 μ M) [20]

^c data not available

Thus it is apparent that the peroxide moiety in these compounds undergoes a cleavage during the reduction process, releasing a free radical which is believed to be a critical step in the antimalarial action of the compounds [2,3,22]. However, in the present case although all the three compounds are irreversibly reduced at the cathode surface due to the presence of the peroxide bond, the near identical reduction potential values of the α - and β -artelinic acids indicate similar bond energies lending support to the modeling data which shows similar distances between the peroxide bond and the H δ_{ax} and H δ_{eq} protons and the ether oxygen atoms and the aromatic ring (Table 5). Inspection of Table 6 indicates that despite similar reduction potential values of the three compounds the antimalarial activity differs significantly between the artelinic acids and arteether and the neurotoxicity between β -artelinic acid and β -arteether. Thus, certain crucial molecular characteristics such as structural requirements and hydrophobicity are important for specific binding to the receptor in order to manifest the desired biological activity.

4 CONCLUSIONS

In summary, the combined NMR, molecular modeling and cyclic voltammetry study on α - and β -artelinic acids, and β -arteether could corroborate remarkably well the structural characteristics of β -artelinic acid and the differences observed in the chemical shifts from NMR experiments. The combined study also correlated the structure and electronic properties of α and β anomers of arteether and artelinic acid with their antimalarial properties. The interaction of the protons near the C10 anomeric carbon atom appears to be particularly significant. The difference in the NMR chemical shifts stems primarily from the difference in interaction between the protons by the anomeric atom C10 in these compounds and the peroxide oxygen atoms remain virtually unaffected. Cyclic voltammetry experiments and the molecular modeling studies are consistent with the NMR results. The near identical redox potential and negative electrostatic potential values of the peroxide oxygen atoms indicate a similar nucleophilic nature of the peroxide bond. The difference that is observed in the anomers is essentially due to the interaction of the aromatic ring with the protons by the C10 atom. The study should aid in the design of more such potent artemisinin analogues with lessened CNS toxicity.

Acknowledgment

The authors acknowledge the financial support of this research by the Department of Army under the Military Infectious Disease Research Program.

Note: The opinions expressed herein are the private views of the authors and are not to be construed as official or reflecting the views of the Department of the Army or the Department of Defense.

5 REFERENCES

- [1] C. W. Jefford, Peroxide Antimalarials, *Adv. Drug Res.* **1997**, 29, 271–325.
- [2] A. J. Lin, A. B. Zikry and D. E. Kyle, Antimalarial activity of new dihydroartemisinin derivatives. 7. 4-(p-substituted phenyl)-4(R or S)-[10(α or β)-dihydroartemisininoxy]butyric acids, *J. Med. Chem.* **1997**, 40, 1396–

- 1400.
- [3] A. J. Lin and R. E. Miller, Antimalarial activity of new dihydroartemisinin derivatives. 6A alkylbenzylic ethers, *J. Med. Chem.* **1995**, *38*, 764–770.
- [4] J. M. Karle and A. J. Lin, Correlation of the crystal structures of diastereomeric artemisinin derivatives with their proton NMR spectra in CDCl₃, *Acta. Cryst.* **1995**, *B51*, 1063–1068.
- [5] R. A. Vishwakarma and R. Mehrotra, Stereoselective synthesis and antimalarial activity of α -artelinic acid from artemisinin, *J Nat Products*, **1992**, *55*, 1142–1144.
- [6] M. F. Summers, L. G. Marzilli and A. Bax, New Insights into the solution behavior of cobalamin, studies of the base-off form of coenzyme B12 using modern two-dimensional nmr methods, *J. Am. Chem. Soc.* **1986**, *108*, 4285–4286.
- [7] R. E. Desjardins, C. J. Canfield, D. E. Haynes and J. D. Chulay, Quantitative assessment of activity in vitro by a semiautomated microdilution technique, *Antimicrob. Agents Chemther.* **1979**, *16*, 710–718.
- [8] J. D. Chulay, J. D. Haynes and C. L. Diggs, Plasmodium falciparum: Assessment of in vitro growth by [³H]hypoxanthine incorporation, *Exp. Parasitol.* **1983**, *55*, 138–146.
- [9] M. R. Smyth and J. G. Vos, Analytical Voltammetry; Elsevier: New York, 1992; vol. 27; pp 16–20.
- [10] SPARTAN, version 5.0, **1997**, Wavefunction, Inc., Irvine, CA.
- [11] M. J. Frisch, G. W. Trucks, H. B. Schlegel, P. M. W. Gill, B. G. Johnson, M. A. Robb, J. R. Cheeseman, T. A. Keith, G. A. Petersson, J. A. Montgomery, K. Raghavachari, M. A. Al-Laham, V. G. Zakrzewski, J. V. Ortiz, J. B. Foresman, J. Cioslowski, B. B. Stefanov, A. Nanayakkara, M. Challacombe, C. Y. Peng, P. Y. Ayala, W. Chen, M. W. Wong, J. L. Andres, E. S. Replogle, R. Gomperts, R. L. Martin, D. J. Fox, J. S. Binkley, D. J. Defrees, J. Baker, J. P. Stewart, M. Head-Gordon, C. Gonzalez and J. A. Pople, **1995**, Gaussian 94 (Revision A.1), Gaussian Inc., Pittsburgh PA.
- [12] Y. Okuno, T. Kamokado, S. Yokoyama and S. Mashiko, Determining the conformation of a phenylene-linked porphyrin dimer by NMR spectroscopy and quantum chemical calculations, *J. Mol. Structure (Theochem)*, **2003**, *631*, 13–20.
- [13] Y. Yamaguchi, Ab initio study of proton chemical shift in supercritical methanol using gas-phase approximation, *J. Phys. Chem. A*, **2001**, *106*, 404–410.
- [14] G. E. Martin and A. S. Zektzer, Two-Dimensional NMR Methods for Establishing Molecular Connectivity, VCH Publishers, 1988, pp 162–344.
- [15] A. Rahman, One and Two Dimensional NMR Spectroscopy, Elsevier, 1989, pp 391–423.
- [16] Quinghaosu antimalarial coordinating research group, *Chin. Med. J.* **1979**, *92*, 811–816.
- [17] I. Leban, L. Golic and M. Japelj, Crystal and molecular structure of qinghaosu: a redetermination, *Acta Pharm. Jugosl.* **1988**, *38*, 71–77.
- [18] A. K. Bhattacharjee and J. M. Karle, Stereoelectronic properties of antimalarial artemisinin analogues in relation to neurotoxicity, *Chem. Res. Toxicol.* **1999**, *12*, 422–428.
- [19] G. Bernardinelli and C. W. Jefford, Computational studies of the structures and properties of potential antimalarial compounds based on the 1,2,4-trioxane ring structure. I. Artemisinin-like molecules, *Intl. J. Quant. Chem., Quant. Bio. Symp.* **1994**, *21*, 117–131.
- [20] D. L. Wesche, M. A. DeCoster, F. C. Tortella, and T. G. Brewer, Neurotoxicity of artemisinin analogs in vitro, *Antimicrob. Agents Chemother.* **1994**, *38*, 1813–1819.
- [21] Q. Du and G. A. Arteca, Modeling lipophilicity from the distribution of electrostatic potential on a molecular surface, *J. Comput. Aided Mol. Des.*, **1996**, *10*, 133–144.
- [22] Y. Chen, C. X. He, S. M. Zhu and H. Y. Chen, Electrocatalytic reduction of artemether by hemin, *J. Electrochem. Soc.* **1997**, *144*, 1891–1894.

Biographies

Apurba K. Bhattacharjee is the Chief Molecular Modeler in the department of medicinal chemistry at the Division of Experimental Therapeutics, Walter Reed Army Institute of Research, Silver Spring, Maryland, U.S.A. After obtaining a Ph.D. degree in physical organic chemistry from the North Eastern Hill University (India) in 1983, Dr. Bhattacharjee undertook postdoctoral research with Professor J.-E. Dubois at the Institut de Topologie et de Dynamique des Systemes de l'Univerite Paris 7 (France) for two and half years and returned to India to teach. He is in the current position since July, 1995. More recently, Dr. Bhattacharjee has collaborated on projects with Professor Jonathan Vennerstrom of College of Pharmacy, University of Nebraska to identify the critical molecular features of the antimalarial, chloroquine, to reverse its resistance to the parasites. Dr. Bhattacharjee has currently undertaken a major research project to identify new antimalarial agents by targeting the fatty acid biosynthetic pathway enzymes of the parasites. He has more than 60 publications in major international peer reviewed journals and three patents. His extracurricular activities involve reading books and articles ranging from different philosophies of the world to religions, and international politics.

David Skanchy received his Ph.D. in Pharmaceutical Chemistry in 1996 from the University of Kansas under the direction of John F. Stobaugh. After completing his degree Dr. Skanchy went on active duty in the U.S. Army assigned to the Walter Reed Army Institute of Research where he served as an associate researcher and later, Department Chief in the Medicinal Chemistry Department. After a final assignment at the Forensic Toxicology Laboratory, Ft. Meade as Deputy Commander, Dr. Skanchy left the Army to accept a commission in the United States Public Health Service and is currently assigned to the Food and Drug Administration, Rockville MD. Dr. Skanchy has published 15 papers in the areas of pharmaceutical analysis, drug metabolism, and drug discovery.

Rickey P. Hicks is a natural product chemist, received his Ph.D. in natural products chemistry from Virginia Commonwealth University under direction of Professor Albert T. Sneden in 1984. After graduation he joined the staff of Nova Pharmaceutical Corporation in Baltimore Maryland. During this time his research focused on the development of novel adenosine antagonists and anti-inflammatory agents. In 1989 he joined the faculty in the Department of Chemistry at Mississippi State University, he was promoted with tenure to Associate Professor in 1994. His research at Mississippi State focused on the application of nuclear magnetic resonance spectroscopy to study the conformation induced onto linear polypeptides by micelles and lipid bilayers. He has graduated two Ph.D. and five masters students. In January 2001, he joined the staff of the Department of Medicinal Chemistry in the Division of Experimental Therapeutics at the Walter Reed Army Institute of Research as the Chief of the Nuclear Magnetic Resonance Analysis Laboratory. He has co-authored over 30 manuscripts and book chapters as well as four patents.